

Published in final edited form as:

Cancer Cell. 2012 March 20; 21(3): 362–373. doi:10.1016/j.ccr.2012.02.010.

Activated ALK Collaborates with MYCN in Neuroblastoma Pathogenesis

Shizhen Zhu^{1,9}, Jeong-Soo Lee^{1,2,9}, Feng Guo¹, Jimann Shin^{1,3}, Antonio R. Perez-Atayde⁴, Jeffery L. Kutok^{5,6}, Scott J. Rodig⁵, Donna S. Neuberg⁷, Daniel Helman¹, Hui Feng¹, Rodney A. Stewart^{1,8}, Wenchao Wang¹, Rani E. George¹, John P. Kanki¹, and A. Thomas Look^{1,*}

¹Department of Pediatric Oncology, Dana-Farber Cancer Institute, Harvard Medical School, Boston MA, 02115, USA

⁴Department of Pathology, Children's Hospital Boston, Harvard Medical School, Boston MA, 02115, USA

⁵Department of Pathology, Brigham and Women's Hospital, Harvard Medical School, Boston MA, 02115, USA

⁷Department of Biostatistics and Computational Biology, Dana-Farber Cancer Institute, Harvard Medical School, Boston MA, 02115, USA

SUMMARY

Amplification of the *MYCN* oncogene in childhood neuroblastoma is often accompanied by mutational activation of *ALK* (anaplastic lymphoma kinase), suggesting their pathogenic cooperation. We generated a transgenic zebrafish model of neuroblastoma in which *MYCN*-induced tumors arise from a subpopulation of neuroblasts that migrate into the adrenal medulla analogue following organogenesis. Coexpression of activated *ALK* with *MYCN* in this model triples the disease penetrance and markedly accelerates tumor onset. *MYCN* overexpression induces adrenal sympathetic neuroblast hyperplasia, blocks chromaffin cell differentiation, and ultimately triggers a developmentally-timed apoptotic response in the hyperplastic sympathoadrenal cells. Coexpression of activated *ALK* with *MYCN* provides prosurvival signals that block this apoptotic response and allow continued expansion and oncogenic transformation of hyperplastic neuroblasts, thus promoting progression to neuroblastoma.

© 2012 Elsevier Inc. All rights reserved

*Correspondence: Thomas.Look@dfci.harvard.edu (A.T.L.).

²Present Address: Korea Research Institute of Bioscience & Biotechnology, Aging Research Center, Daejeon 305-806, Korea.

³Present Address: Department of Developmental MANUS Biology, Washington University School of Medicine, Saint Louis, MO 63110, USA.

⁶Present Address: Molecular Pathology, Infinity Pharmaceuticals, Cambridge, MA 02139, USA.

⁸Present Address: Huntsman Cancer Institute, Department of Oncological Sciences, University of Utah, Salt Lake City, UT 84112, USA.

⁹These authors contributed equally to this work.

Publisher's Disclaimer: This is a PDF file of an unedited manuscript that has been accepted for publication. As a service to our customers we are providing this early version of the manuscript. The manuscript will undergo copyediting, typesetting, and review of the resulting proof before it is published in its final citable form. Please note that during the production process errors may be discovered which could affect the content, and all legal disclaimers that apply to the journal pertain.

SUPPLEMENTAL INFORMATION Supplemental information includes Supplemental Experimental Procedures, 7 figures and one table and can be found with this article online at.

INTRODUCTION

Neuroblastoma is a childhood solid tumor that arises in the peripheral sympathetic nervous system (PSNS), typically in the adrenal medulla or paraspinal ganglia, during embryogenesis (Brodeur, 2003; Maris, 2011). When disseminated at diagnosis in older children, the disease carries a very poor prognosis despite the use of intensive therapies. Amplification of the *MYCN* oncogene is found in tumor cells from about 20% of neuroblastoma patients and is the most reliable marker of a poor prognosis (Brodeur, 2003; Maris et al., 2007). Overexpression of *MYCN* in the PSNS of transgenic mice, using the rat tyrosine hydroxylase (*TH*) promoter, results in tumors that closely resemble human neuroblastoma arising in the sympathetic ganglia (Chesler et al., 2011; Weiss et al., 1997), indicating that aberrant expression of *MYCN* promotes the development of this tumor *in vivo*.

The anaplastic lymphoma kinase (*ALK*) gene encodes a receptor tyrosine kinase that is normally expressed at high levels in the nervous system and was originally identified as a fusion protein with nucleophosmin in cases of anaplastic large cell lymphoma (Morris et al., 1994). Activation of *ALK* can regulate cellular proliferation, differentiation and apoptosis via a number of different signaling pathways, including PI3K/AKT, RAS/MAPK and STAT3, but its precise physiologic role remains elusive (Chiarle et al., 2008; Palmer et al., 2009). Recently, we and others reported that amplification of the *ALK* gene occurs only in *MYCN*-amplified primary neuroblastomas and that within this group about 15% of cases have *ALK* amplification (George et al., 2008; Mosse et al., 2008). Activating *ALK* mutations were also identified in both familial and sporadic neuroblastoma cases, including but not limited to a subset with *MYCN* amplification, further implicating this kinase in neuroblastoma pathogenesis (Chen et al., 2008; George et al., 2008; Janoueix-Lerosey et al., 2008; Mosse et al., 2008). Mechanisms through which signaling by aberrantly activated *ALK* cooperates with *MYCN* overexpression to enhance neuroblastoma development remain undefined, posing a major obstacle to the development of effective targeted treatments for this devastating disease.

We have generated a transgenic zebrafish model in which overexpression of human *MYCN* in the PSNS induces tumors in the fish analogue of the adrenal medulla that closely resemble human neuroblastoma. Using this model system, we undertook studies to explore mechanistically the interaction between mutationally activated *ALK* and *MYCN* overexpression during neuroblastoma pathogenesis in the PSNS.

RESULTS

Transgenic EGFP expression in the PSNS

We first isolated a 5.2-kb promoter fragment upstream of the coding sequence of the zebrafish dopamine- β -hydroxylase gene (*d β h*), which encodes the rate-limiting enzyme for noradrenalin synthesis. This fragment was used to drive expression of enhanced green fluorescent protein (EGFP) in a stable zebrafish transgenic line, *Tg(d β h:EGFP)*, designated D β H in this article. In juvenile and adult transgenic zebrafish, EGFP was specifically expressed by sympathetic neurons of the superior cervical ganglia (Figures 1A–1C), the first sympathetic ganglion to develop in early embryogenesis, and by each sequential segmental ganglion of the sympathetic chain (Figures 1A, 1B and 1D). EGFP was also expressed by sympathoadrenal cells of the interrenal gland (Figures 1A, 1B and 1E), the zebrafish equivalent of the human adrenal gland (Hsu et al., 2003). In the interrenal gland, the EGFP-expressing cells can be visualized within a discrete region in the ventral aspect of the head kidney, intermixed with adrenal cortical cells that are TH- and EGFP-negative (Figure 1E). The specificity of EGFP expression for sympathoadrenal cells when driven by the *d β h*

promoter fragment is demonstrated by coexpression of endogenous TH (Figures 1C–1E), another enzyme expressed by sympathetic neurons and chromaffin cells (An et al., 2002; O'Brien et al., 2004).

Zebrafish expressing *MYCN* develop neuroblastoma

Using a coinjection strategy (Langenau et al., 2008), we generated a stable transgenic zebrafish line, *Tg(dβh:EGFP-MYCN)*, designated MYCN in this article, that overexpresses the human *MYCN* gene fused to EGFP under control of the *dβh* promoter. In MYCN transgenic fish the expansion of cells expressing EGFP as tumors developed was readily detectable in living fish by immunofluorescence microscopy (Figure 2A). EGFP⁺ tumor masses were found in the anterior abdomen, corresponding to the interrenal gland, and were composed of small, undifferentiated, round-tumor cells with hyperchromatic nuclei, often forming nests (Figure 2B). Tumor cells were strongly immunoreactive for TH and the pan-neuronal markers Hu and Synaptophysin (Figure 2C), indicating their PSNS-related neuronal origin (Gould et al., 1986; Marusich et al., 1994; Teitelman et al., 1979). Normal interrenal chromaffin cells also expressed TH, but not Hu or Synaptophysin (Figure 2C), indicating that the neuroblastomas arose from sympathetic neuroblast precursors and not chromaffin cells, as is the case in human neuroblastoma (Figure 2E).

Neuroblastoma is frequently considered in the differential diagnosis of malignant small round-cell tumors of childhood, and electron microscopy is a helpful tool for distinguishing among these malignancies. A diagnosis of neuroblastoma can be established ultrastructurally by demonstrating the presence of neurosecretory granules within the cytoplasm or cytoplasmic processes of tumor cells (Figure 2E) (Mierau et al., 1998). These neurosecretory granules were evident in the tumors we identified in the zebrafish (Figure 2D), strengthening their association with childhood neuroblastoma. The histopathological, immunohistochemical and ultrastructural features of neuroblastoma are shown in Figure 2E, to illustrate their similarities with those of neuroblastomas induced by *MYCN* overexpression in zebrafish (Figures 2B–2D) (Hoshi et al., 2008; Mierau et al., 1998; Molenaar et al., 1990; Taxy, 1980; Tornoczky et al., 2007). These findings support our use of this model to investigate activated ALK as a contributor to *MYCN*-driven tumorigenesis.

ALK accelerates *MYCN*-induced neuroblastoma

We and others have implicated activating mutations of *ALK* in the pathogenesis of neuroblastoma, including cases that also show *MYCN* amplification (De Brouwer et al., 2010; George et al., 2008; Mosse et al., 2008). To address whether *ALK* and *MYCN* genetically interact during neuroblastoma induction, we generated a second stable transgenic zebrafish line that expresses the human *ALK* gene harboring the *F1174L* mutation, one of the most prevalent somatic activating mutations found in neuroblastoma patients and human cell lines (Chen et al., 2008; George et al., 2008). The *dβh:EGFP* and *dβh:ALKF1174L* constructs were coinjected into zebrafish embryos at the one-cell stage to generate a transgenic line expressing both the EGFP and activated *ALK* transgenes, *Tg(dβh:EGFP;dβh:ALKF1174L)*, designated ALK in this article. EGFP was specifically expressed by sympathoadrenal cells in the interrenal gland of the ALK transgenic fish at 5 weeks postfertilization (wpf), and *ALK* was coexpressed with EGFP by the same cells (Figure S1A). This transgenic line was bred to the *MYCN* heterozygous transgenic line, and the offspring were monitored for evidence of tumors. All of the expected genotypes were represented in the offspring of this cross: i) *MYCN*, ii) *ALK*, iii) *MYCN*;*ALK*, and iv) wild-type (WT) AB fish lacking either transgene. A tumor watch was performed on a total of 1156 sorted offspring. The fish were isolated in individual tanks as soon as tumors appeared; and were sacrificed for molecular and pathologic analyses when there was evidence of tumor progression.

The first 23 tumors arose between 5–7 weeks of age, and all had the compound transgenic genotype, MYCN;ALK (Figure 3A). The expression of MYCN and ALK proteins and *ALK* RNA was confirmed in the tumors of these compound transgenic fish by immunohistochemical and RT-PCR analyses, respectively (Figures S1B and S1C). Tumors continued to arise after 9 weeks of age in both the MYCN-only and the MYCN;ALK compound transgenic lines, but their rate of induction was much higher in the latter group (Figure 3A). Tumor penetrance in the MYCN;ALK compound transgenic fish was also much higher: 55.6% vs. 17.3% for the MYCN transgenic fish ($p < 0.0001$; Figure 3A). Although germline mutations of *ALK* cause hereditary neuroblastoma (Mosse et al., 2008), tumors did not develop in fish expressing this transgene alone over the 6-month monitoring period (Figure 3A). Tumors in the compound transgenic fish arose in the interrenal gland, as did those in the MYCN fish, and these tumors were comparable histologically, immunohistochemically, and ultrastructurally (Figure S2) to human neuroblastoma (Figure 2E).

To control for possible founder effects in our transgenic lines, and to examine whether overexpression of wild-type *ALK* (ALKWT) as well as mutationally activated *ALK* could collaborate with MYCN in neuroblastoma pathogenesis, we overexpressed either activated human *ALK* or human *ALKWT* in MYCN fish. For this experiment, we coinjected the following constructs into the one-cell stage of MYCN transgenic and control embryos: i) *dβh-ALKF1174L* with *dβh-mCherry*, ii) *dβh-ALKWT* with *dβh-mCherry*, or iii) *dβh-mCherry* alone. We have shown that this coinjection strategy results in cointegration into DNA and coexpression of the two coinjected transgenes as mosaics in a subset of cells in ~50% of the injected embryos (Langenau et al., 2008). Thus, the expression of mCherry served as a marker for the coexpression of *ALK* in tissues of the mosaic primary injected animals. When these animals were monitored for the tumor onset, neuroblastomas were not observed in any of the siblings that did not inherit the *MYCN* transgene and were injected with either the *ALKWT* or *ALKF1174L* transgenes, emphasizing that overexpression of *MYCN* is required for tumorigenesis in this model. Eight tumors arose by 9 wpf in the MYCN fish coinjected with *dβh-ALKF1174L* and *dβh-mCherry* (Figures 3B and S3A), while none were observed by 9 wpf in the MYCN line coinjected with *dβh-ALKWT* and *dβh-mCherry* ($p = 0.002$; Figures 3B and S3B) or with *dβh-mCherry* alone ($p = 0.007$; Figures 3B and S3C). In addition, four tumors in the MYCN line coinjected with *dβh-ALKWT* and *dβh-mCherry* and five tumors in the MYCN line injected with *dβh-mCherry* alone were identified after 11 wpf (Figure 3B), similar to the time of tumor onset in the uninjected MYCN line (Figure 3A). These findings show that activated *ALK* cooperates with *MYCN* overexpression to accelerate the onset of neuroblastoma, regardless of the integration site in individual mosaic animals, and that overexpression of *ALKWT* at the levels driven by the *dβh* promoter does not appear to collaborate with *MYCN* to induce neuroblastoma in this model system.

MYCN-induced loss of sympathoadrenal cells

To investigate the cellular basis for MYCN-induced neuroblastoma and its modification by constitutively activated *ALK*, we examined the development of sympathoadrenal cells in i) DβH, ii) MYCN, iii) *ALK*, and iv) MYCN;ALK transgenic fish during the embryonic and larval stages. During normal development, PSNS cells arise from the neural crest and migrate ventrally to locations adjacent to the dorsal aorta (Huber, 2006). After forming the superior cervical ganglia, a subset of sympathoadrenal cells migrate further to invade the mesonephros and differentiate to form chromaffin cells in the interrenal gland (An et al., 2002; Huber, 2006; Stewart et al., 2004). We identified cells of the developing superior cervical ganglia at 80 hours postfertilization (hpf) in living DβH transgenic fish and in whole-mount *in situ* hybridization preparations with *dβh*- and *th*- riboprobes (Figure 4A),

indicating that EGFP expression in the developing embryonic PSNS of this transgenic line recapitulates the normal endogenous expression patterns of *dβh* and *th* (Figure 4A). By 80 hpf, EGFP was apparent in the superior cervical ganglia, as well as in non-PSNS dopaminergic neurons, such as the medulla oblongata and cranial ganglia (Figure 4A). By contrast, most MYCN transgenic embryos (~80%) failed to express a detectable level of EGFP fused to human MYCN in the superior cervical ganglia at 80 hpf, even though the fusion protein was clearly expressed in non-PSNS tissues (Figure 4B), and in most animals, the absence of detectable sympathoadrenal cells persisted through 10 dpf (Figure S4C). The lack of EGFP expression is consistent with the markedly reduced numbers of sympathoadrenal cells in MYCN embryos indicated by the loss of cells with endogenous *th* and *dβh* RNA expression by whole-mount *in situ* hybridization (Figures 4B vs. 4A). Because *th* and *dβh* are markers for differentiated sympathoadrenal cells, the absence of cells expressing *EGFP-MYCN* under control of the *dβh* promoter could reflect either MYCN-induced apoptosis or an arrest in sympathoadrenal progenitor cell differentiation.

To distinguish between these possibilities, we first performed TUNEL and anti-activated Caspase-3 staining on sections of 36, 51 and 72 hpf MYCN vs. DβH transgenic fish. We found no evidence of TUNEL- or anti-activated Caspase-3-positive cells in the superior cervical ganglia or regions where sympathoadrenal cells would be expected to form (Figure S5; data not shown), suggesting that the absence of detectable sympathoadrenal cells is not due to cell death, but rather to a failure to initiate the PSNS developmental program at this early time in development. To test this possibility, we performed whole-mount *in situ* hybridization at 54 hpf and 80 hpf for expression of the *phox2b*, *zash1a* and *AP-2 alpha* (*tfap2a*) genes, which encode transcription factors required for sympathoadrenal cell specification and maintenance (Figure 5) (Guillemot et al., 1993; Lucas et al., 2006; Pattyn et al., 1999). Each of these sympathoadrenal cell progenitor markers was readily detectable in the superior cervical ganglia region of control embryos, but undetectable in MYCN transgenic embryos at these stages, indicating that specification of the earliest identifiable sympathoadrenal cell progenitors was blocked by expression of the *EGFP-MYCN* fusion gene. The suppression of sympathoadrenal cell development by *EGFP-MYCN* appears to be tissue-specific, because expression of the *EGFP-MYCN* by non-PSNS dopaminergic neuronal cells in these embryos was largely unaffected, including expression by cells of the locus coeruleus, medulla oblongata, and cranial ganglia (Figures 4B vs. 4A and S4C).

To investigate the possibility that neuroblastoma might arise from residual EGFP-MYCN+ sympathoadrenal cells that can be identified at 3 dpf in approximately 20% of the transgenic embryos, we analyzed these embryos in more detail at 5 dpf. At this time, neurons of the superior cervical ganglia in control DβH transgenic fish express EGFP and are both TH+ and Hu+ (arrows in Figure S4A), whereas chromaffin cells lose Hu expression as they differentiate into chromaffin cells, reflecting a loss of their neuronal phenotype (arrowheads in Figure S4A). Interestingly, the small populations of EGFP+ cells observed in the superior cervical ganglia of MYCN animals were heterogeneous in their immunoreactivity patterns, including cells that were TH+/Hu- (arrowheads in Figure S4B), TH-/Hu- (double arrowheads in Figure S4B), or TH+/Hu+ (data not shown). However, these residual cells did not appear to contribute to neuroblastoma development, as there was no difference in the time of disease onset in the 20% of fish that had small numbers of residual cells at 5 dpf compared to the majority of MYCN transgenic fish, which lacked detectable cells in the superior cervical ganglia (Table S1).

Expression of mutant *ALK F1174L* in ALK transgenic fish did not affect the development of sympathoadrenal cells, as shown by EGFP fluorescence and expression of the *th* and *dβh* RNAs (Figures 4C and S4C). Furthermore, the expression of activated ALK in the presence of MYCN in MYCN;ALK transgenic embryos did not rescue the loss of sympathoadrenal

cells observed in the *MYCN* transgenic embryos (Figures 4D and S4C). Thus, although activated *ALK* clearly cooperates with *MYCN* in tumorigenesis, this interplay does not depend on any ability of *ALK* to reverse the pronounced *MYCN*-induced suppression of sympathoadrenal cell development during early embryonic and larval stages.

Hyperplastic *Hu*⁺ cells in the interrenal gland

Analysis of the PSNS during the first 10 days of life in *MYCN* transgenic zebrafish revealed the profound capacity of high level of *MYCN* to suppress the development of sympathoadrenal cells, but did not provide any insight into why these transgenic fish developed neuroblastoma. Because the first tumors arose in *MYCN*;*ALK* transgenic fish between 5–7 wpf, we examined the interrenal gland of *MYCN* transgenic zebrafish beginning at 3 wpf to identify the cells that give rise to neuroblastoma. In *DβH* control animals, we observed *GFP*⁺/*Hu*⁺/*TH*⁺ neuroblast cells in both the mediolateral (Figure 6A) and lateral regions of the developing interrenal gland (Figure S6). The number of *Hu*⁺ neuroblasts quantified from sections through both interrenal gland regions remained low between 3 and 7 wpf (Figure 6B); *Hu*⁺ cell numbers in *ALK* transgenic fish were comparable to those in controls (Figure 6B). By contrast, the numbers of *Hu*⁺ neuroblasts were significantly increased in *MYCN* transgenic fish, as compared to those in controls at 3 wpf (Figure 6B, *p*=0.03). In 9 of 16 *MYCN* transgenic fish examined, the numbers of *Hu*⁺ neuroblasts were markedly increased at 5 wpf (Figure 6A and 6B, *p*=0.004). However, at 7 wpf, 11 of 16 *MYCN* fish lacked detectable *Hu*⁺ neuroblasts in the interrenal gland (Figure 6B), indicating that during this 2-week period these cells were either eliminated or had differentiated, thus losing their expression of the neuronal marker *Hu*. In *MYCN*;*ALK* compound transgenic fish the numbers of *Hu*⁺ cells also increased during the 3 to 5-week period, but in contrast to transgenic fish expressing *MYCN* alone, the *Hu*⁺ cell numbers continued to increase in 6 of 12 fish at 7 wpf (Figure 6B, *p*=0.03). Thus, *Hu*⁺ cells continue to expand in only a small fraction of transgenic animals expressing *MYCN* alone after 5 wpf, while a much higher fraction of the double transgenic *MYCN*;*ALK* animals showed progressive expansion of *Hu*⁺ cells, mirroring the much higher fraction of these animals that develop fully transformed neuroblastoma (Figure 3A).

To assess the effects of *MYCN* and activated *ALK* expression on the differentiation of *Hu*⁺, *TH*⁺ neuroblast into *Hu*⁻, *TH*⁺ adrenal chromaffin cells, we quantified the numbers of *Hu*⁻, *GFP*⁺ cells within the interrenal gland of each of the zebrafish lines over time. We found increasing numbers of these cells between 3 to 7 wpf in both control *DβH* and *ALK* transgenic zebrafish, indicating the differentiation of the *Hu*⁺ neuroblast precursors into chromaffin cells (Figures 7A–7C). By contrast, the *Hu*⁻, *GFP*⁺ chromaffin cells did not increase normally and remained at very low levels between 3 to 7 wpf in *MYCN*-overexpressing fish relative to control animals, regardless of whether the fish also expressed the activated *ALK* transgene (Figures 7A–7C). At 7 wpf, we identified two *MYCN* transgenic fish and two *MYCN*;*ALK* fish with some expansion of *Hu*⁻/*TH*⁺ chromaffin cells (Figure 7C). Thus, in a small subset of *MYCN*-overexpressing fish, the sympathoadrenal cells manage to differentiate, lose the *Hu* neuronal marker and expand at 7 weeks of age despite activated *ALK* overexpression. The chromaffin cell expansion seems to be self-limited, because all of the tumors that arise in these fish express the *Hu* pan-neuronal marker (Figures 2C and S2C).

To determine whether the loss of *Hu*⁺ cells in the transgenic fish expressing *MYCN* alone between 5 and 7 wpf was due to apoptotic cell death, we assessed the expression of activated Caspase-3 as an indicator of apoptotic cell death. An important difference was observed at 5.5 wpf: transgenic fish expressing *MYCN* alone showed significant numbers of apoptotic cells coexpressing *Hu* and activated Caspase-3 (Figures 8B, 8C and S7C), providing the basis for the profound loss of these cells by 7 wpf. By contrast, in *MYCN*;*ALK* transgenic

fish, we rarely observed apoptotic cells expressing both Hu and activated Caspase-3 (Figures 8B, 8C and S7D), consistent with the continued increase in Hu⁺ cell numbers at 7 wpf in this group (Figure 6B). Neuroblastomas that develop in MYCN transgenic animals coexpress GFP, TH and Hu, regardless of whether the animals also express the activated *ALK* transgene. Thus, the expanding neuroblast cell populations that we identified at 7 wpf in MYCN transgenic animals appear to give rise to fully transformed tumors a few weeks later, and a fraction of the fish with these hyperplastic precursors was markedly increased by coexpression of activated *ALK*, accounting for the increased penetrance of neuroblastoma in the compound transgenic line (Figure 3A). Taken together, these findings indicate that overexpression of *MYCN* prevents the differentiation of neuroblast precursors into adrenal chromaffin cells, and induces a developmentally-timed apoptotic response at 5.5 wpf in most MYCN transgenic fish. However, concomitant expression of activated *ALK* in these cells promotes cell survival without altering the MYCN-induced block in differentiation, resulting in the continued accumulation of Hu⁺ neuroblasts that culminates in the development of highly penetrant, fully transformed neuroblastoma.

DISCUSSION

Early in the embryogenesis of our transgenic zebrafish, *MYCN* overexpression results in a profound loss of neural crest-derived cells within the sympathoadrenal cell lineage. Nevertheless, these animals can develop neuroblastoma, and both the onset and penetrance of the disease are markedly enhanced by coexpression of a transgene encoding the activated *ALK* receptor tyrosine kinase. Thus, our zebrafish model clearly demonstrates a synergistic relationship between these two genes in neuroblastoma pathogenesis. Using multiparameter confocal microscopy and immunohistochemistry to examine embryos throughout early development, we show that MYCN-induced neuroblastoma does not arise from the earliest cells populating the superior cervical ganglia (3–6 dpf), but rather from neuroblasts that migrate into the interrenal gland later in development (~21 dpf), after the kidney has developed. The interrenal gland is the zebrafish equivalent of the human adrenal gland, and sympathoadrenal precursors in the interrenal gland coexpress neuronal-specific Hu proteins and the catecholaminergic enzymes TH and D β h. The interrenal gland origin of neuroblastoma in zebrafish recapitulates the adrenal medullary site of origin observed in approximately half of the children with this tumor (Janoueix-Lerosey et al., 2010), in contrast to the murine *MYCN* transgenic model, where tumors arise from hyperplastic neuroblasts predominately in the sympathetic cervical ganglia complex and the superior cervical ganglia (Alam et al., 2009; Hansford et al., 2004). In the study by Hansford and coworkers (Hansford et al., 2004), these hyperplastic neuroblasts regressed due to apoptotic cell death in normal and hemizygous transgenic animals, but frequently progressed to fully transformed neuroblastoma in homozygous transgenic animals. The similarities and differences between the murine and zebrafish transgenic models afford complementary opportunities to investigate mechanisms underlying sympathoadrenal cell transformation within the distinct anatomical locations that comprise the PSNS.

Using the zebrafish model, we now show that expression of aberrantly activated *ALK* potentiates the oncogenic effects of *MYCN* by blocking the apoptotic death of *MYCN*-overexpressing sympathoadrenal neuroblasts. The death of these cells occurs within a well-defined developmental window, 5.5 wpf, indicating that although overexpression of *MYCN* causes aberrant expansion of these cells from 3 to 5 wpf, it also triggers an apoptotic response at 5.5 wpf. By monitoring the appearance of more differentiated adrenal chromaffin cell numbers in animals of each genotype, we show that these *MYCN*-overexpressing neuroblasts fail to differentiate, resulting in reduced numbers of Hu⁻, TH⁺, D β h⁺ chromaffin cells. The MYCN-induced apoptotic response in these cells does not seem to result from the types of constitutive MYC- or MYCN-induced apoptotic signaling that has

been described by others (Fanidi et al., 1992; Finch et al., 2006; Nilsson et al., 2003), because the *MYCN*-overexpressing immature neuroblasts in our transgenic fish do not undergo apoptosis during their expansion to 5 wpf. Rather, the apoptotic death of these cells appears to result from a conflict between aberrant proliferative signals emanating from overexpressed *MYCN* and other developmentally timed signals that specify chromaffin cell fate. Thus, activated ALK provides a cell survival signal that blunts the apoptotic response of *MYCN*-overexpressing neuroblasts at this juncture in development, but does not restore the ability of these cells to differentiate. For the 17% of *MYCN*-only transgenic fish that develop tumors, it is likely that additional genetic alterations cooperate with this oncogene to contribute to neuroblastoma transformation. Nevertheless, we did not detect somatic missense mutations within the tyrosine kinase domain of the zebrafish *alk* gene in ten tumors from *MYCN*-only transgenic fish, or a loss of *capsase-8* expression, which has been implicated in the pathogenesis of human neuroblastoma with *MYCN* amplification. Thus, mutations or epigenetic events that activate prosurvival pathways other than those mediated by *alk* activation or *capsase-8* loss of function appear to interact with *MYCN* overexpression in these tumors.

The mutant *ALK (F1174L)* gene that we expressed in our zebrafish model has not been observed in the germline of human patients with familial neuroblastoma. This suggests that it may generate signals that are incompatible with normal human embryogenesis, making it more potent than the *R1275Q* mutation, the most common neuroblastoma. In our transgenic zebrafish model, the mutation in familial *ALK (F1174L)* mutation is tolerated in the germline, presumably because it is driven in a tissue-specific manner in sympathoadrenal cells by the *dβh* promoter. In our model system, overexpression of *MYCN* is required for the development of neuroblastoma and activated *ALK* expression is not sufficient, even though germline mutations of *ALK* can function as an initiating event in human neuroblastoma, and these tumors may or may not have *MYCN* amplification (Mosse et al., 2008). Further study in the zebrafish model will be required to determine whether mutational events other than *MYCN* overexpression can cooperate with activated ALK to induce neuroblastoma.

The potent anti-apoptotic effect of activated *ALK* expression combined with *MYCN* overexpression might be expected to mediate greater resistance to drug-induced apoptosis and a poorer outcome for patients whose tumors have both amplified *MYCN* and an activating *ALK* mutation. This prediction gains support from a recent meta-analysis of *ALK* mutations in childhood neuroblastoma with *MYCN* amplification, which showed that the mutant *ALK (F1174L)* gene is expressed in a high proportion of childhood tumors with *MYCN* amplification, and that these children have an especially poor outcome (De Brouwer et al., 2010). A new ALK small molecule inhibitor, crizotinib (PF-02341066), has produced encouraging results in a recently completed phase II trial for patients with non-small-cell lung cancer that harbors activating *ALK* rearrangements, including *EML4-ALK* or *RANBP2-ALK* (Butrynski et al., 2010; Kwak et al., 2010; Sasaki et al., 2010), and has been approved by the FDA for use in patients with such tumors. A phase I trial of the same inhibitor was recently initiated in children with solid tumors, including those with neuroblastoma harboring either mutated or amplified *ALK*. Despite these advances, a recent report indicates that the *ALK (F1174L)* mutation confers resistance to crizotinib (Sasaki et al., 2010), which will likely interfere with the activity of this drug against neuroblastomas harboring this mutation. We suggest that the zebrafish model described in this article will provide a useful platform for testing alternative small molecule inhibitors of *F1174L*-activated *ALK*, or key targets within its downstream pathways, to improve the treatment of this aggressive form of childhood neuroblastoma.

EXPERIMENTAL PROCEDURES

Zebrafish

Zebrafish were the AB background strain. Embryos were staged according to Kimmel et al. (Kimmel et al., 1995). All zebrafish studies and maintenance of the animals were in accord with Dana-Farber Cancer Institute IACUC-approved protocol #02-107.

DNA constructs for transgenesis

The 5.2-kb promoter region of the *dβh* gene was amplified by PCR from a zebrafish BAC clone and subcloned into vectors to drive the expression of several genes, including *Tg(dβh:EGFP)*, *Tg(dβh:EGFP-MYCN)* and *Tg(dβh:EGFP;dβh:ALKF1174L)* in tissues normally expressing the *dβh* gene. Embryos were injected with these DNA constructs at the one-cell stage and grown to adulthood. Fin clips from the offspring were genotyped for the stable integration and germline transmission of the transgenes. The *Tg(dβh:EGFP)*, *Tg(dβh:EGFP-MYCN)* and *Tg(dβh:EGFP;dβh:ALKF1174L)* zebrafish lines are designated the “DβH”, “MYCN” and “ALK” transgenic line in this manuscript, respectively.

Tumor watch of transgenic fish

MYCN and ALK heterozygous transgenic fish were crossed, and offspring were screened every 2 weeks starting from 5 wpf for fluorescent EGFP-expressing cell masses indicative of tumors. In addition, for Figure 3B, either activated human *ALK* or wild-type human *ALK* (*ALKWT*) were overexpressed in MYCN fish as mosaics by coinjecting the following constructs into the one-cell stage of MYCN transgenic and control embryos: i) *dβh-ALKF1174L* with *dβh-mCherry*, ii) *dβh-ALKWT* with *dβh-mCherry* or iii) *dβh-mCherry* alone. The primary injected embryos were raised and monitored for the onset of tumorigenesis as described above. Fish with tumors were separated and analyzed further by H&E staining and immunohistochemical assays.

RNA *in situ* hybridization, cryosectioning, paraffin sectioning and immunostaining

RNA *in situ* hybridization assays were performed according to Thisse and Thisse (Thisse et al., 2008). Constructs for making RNA probes to detect *dβh*, *th*, *phox2b* and *tfap2a* expression have been described (Stewart et al., 2006). Fish were fixed with 4% paraformaldehyde and embedded in agar/sucrose or paraffin blocks for cryosectioning or paraffin sectioning, respectively. Sections were immunostained by conventional protocols (Macdonald, 1999) using antibodies against GFP, TH, Hu, Synaptophysin and ALK.

Electron microscopy and imaging

Transmission electron microscopy (TEM) of tumor cells was carried out at the Harvard Medical School EM Facility with a Tecnai™ G² Spirit BioTWIN scope equipped with an AMT 2k CCD camera. A Zeiss LSM 510 META confocal microscope and Leica SP5X Laser Scanning Confocal Microscope were used to capture fluorescent images at high magnification, while a Leica M420 stereoscopic microscope captured bright field and low-magnification fluorescent images. Images were processed with Leica LAS AF Lite, Improvision Openlab v5 and Adobe Photoshop software.

Additional methods are presented in Supplemental Experimental Procedures.

Supplementary Material

Refer to Web version on PubMed Central for supplementary material.

Acknowledgments

This work was supported by a grant CA104605 from the National Cancer Institute, NIH (A. T. L.), a Young Investigator Award from Children's Tumor Foundation and Neuroblastoma Foundation, a fellowship from the Friends for Life (S. Z. and R. E. G.), a fellowship from the Hope Street Kids Foundation (J. S. L.), a fellowship from Durand Family Fund for Pediatric Neuroblastoma Research (J. S. L.), a fellowship from the David A. Abraham Fund and Pediatric Low Grade Astrocytoma Foundation (J. S.), an award K99CA134743 from the National Cancer Institute, NIH (H. F.), an award R00 NS058608 from NIH/NINDS (R. A. S.) and a grant from the National Institutes of Health and the Children's Oncology Group (R. E. G.). We thank John Gilbert for editing the manuscript and critical comments, and Greg Molind, Lu Zhang, Derek Walsh and John P. Lyons for excellent care of our zebrafish facility.

REFERENCES

- Alam G, Cui H, Shi H, Yang L, Ding J, Mao L, Maltese WA, Ding HF. MYCN promotes the expansion of Phox2B-positive neuronal progenitors to drive neuroblastoma development. *Am J Pathol.* 2009; 175:856–866. [PubMed: 19608868]
- An M, Luo R, Henion PD. Differentiation and maturation of zebrafish dorsal root and sympathetic ganglion neurons. *J Comp Neurol.* 2002; 446:267–275. [PubMed: 11932942]
- Brodeur GM. Neuroblastoma: biological insights into a clinical enigma. *Nat Rev Cancer.* 2003; 3:203–216. [PubMed: 12612655]
- Butrynski JE, D'Adamo DR, Hornick JL, Dal Cin P, Antonescu CR, Jhanwar SC, Ladanyi M, Capelletti M, Rodig SJ, Ramaiya N, et al. Crizotinib in ALK-rearranged inflammatory myofibroblastic tumor. *N Engl J Med.* 2010; 363:1727–1733. [PubMed: 20979472]
- Chen Y, Takita J, Choi YL, Kato M, Ohira M, Sanada M, Wang L, Soda M, Kikuchi A, Igarashi T, et al. Oncogenic mutations of ALK kinase in neuroblastoma. *Nature.* 2008; 455:971–974. [PubMed: 18923524]
- Chesler L, Weiss WA. Genetically engineered murine models - Contribution to our understanding of the genetics, molecular pathology and therapeutic targeting of neuroblastoma. *Semin Cancer Biol.* 2011
- Chiarle R, Voena C, Ambrogio C, Piva R, Inghirami G. The anaplastic lymphoma kinase in the pathogenesis of cancer. *Nat Rev Cancer.* 2008; 8:11–23. [PubMed: 18097461]
- De Brouwer S, De Preter K, Kumps C, Zbrocki P, Porcu M, Westerhout EM, Lakeman A, Vandesompele J, Hoebeek J, Van Maerken T, et al. Meta-analysis of neuroblastomas reveals a skewed ALK mutation spectrum in tumors with MYCN amplification. *Clin Cancer Res.* 2010; 16:4353–4362. [PubMed: 20719933]
- Fanidi A, Harrington EA, Evan GI. Cooperative interaction between c-myc and bcl-2 proto-oncogenes. *Nature.* 1992; 359:554–556. [PubMed: 1406976]
- Finch A, Prescott J, Shchors K, Hunt A, Soucek L, Dansen TB, Swigart LB, Evan GI. Bcl-xL gain of function and p19 ARF loss of function cooperate oncogenically with Myc in vivo by distinct mechanisms. *Cancer Cell.* 2006; 10:113–120. [PubMed: 16904610]
- George RE, Sanda T, Hanna M, Frohling S, Luther W 2nd, Zhang J, Ahn Y, Zhou W, London WB, McGrady P, et al. Activating mutations in ALK provide a therapeutic target in neuroblastoma. *Nature.* 2008; 455:975–978. [PubMed: 18923525]
- Gould VE, Lee I, Wiedenmann B, Moll R, Chejfec G, Franke WW. Synaptophysin: a novel marker for neurons, certain neuroendocrine cells, and their neoplasms. *Hum Pathol.* 1986; 17:979–983. [PubMed: 3093369]
- Guillemot F, Lo LC, Johnson JE, Auerbach A, Anderson DJ, Joyner AL. Mammalian achaete-scute homolog 1 is required for the early development of olfactory and autonomic neurons. *Cell.* 1993; 75:463–476. [PubMed: 8221886]
- Hansford LM, Thomas WD, Keating JM, Burkhart CA, Peaston AE, Norris MD, Haber M, Armati PJ, Weiss WA, Marshall GM. Mechanisms of embryonal tumor initiation: distinct roles for MycN expression and MYCN amplification. *Proc Natl Acad Sci U S A.* 2004; 101:12664–12669. [PubMed: 15314226]

- Hoshi N, Hitomi J, Kusakabe T, Fukuda T, Hirota M, Suzuki T. Distinct morphological and immunohistochemical features and different growth rates among four human neuroblastomas heterotransplanted into nude mice. *Med Mol Morphol*. 2008; 41:151–159. [PubMed: 18807141]
- Hsu HJ, Lin G, Chung BC. Parallel early development of zebrafish interrenal glands and pronephros: differential control by wt1 and ff1b. *Development*. 2003; 130:2107–2116. [PubMed: 12668625]
- Huber K. The sympathoadrenal cell lineage: specification, diversification, and new perspectives. *Dev Biol*. 2006; 298:335–343. [PubMed: 16928368]
- Janoueix-Lerosey I, Lequin D, Brugieres L, Ribeiro A, de Pontual L, Combaret V, Raynal V, Puisieux A, Schleiermacher G, Pierron G, et al. Somatic and germline activating mutations of the ALK kinase receptor in neuroblastoma. *Nature*. 2008; 455:967–970. [PubMed: 18923523]
- Janoueix-Lerosey I, Schleiermacher G, Delattre O. Molecular pathogenesis of peripheral neuroblastic tumors. *Oncogene*. 2010; 29:1566–1579. [PubMed: 20101209]
- Kimmel CB, Ballard WW, Kimmel SR, Ullmann B, Schilling TF. Stages of embryonic development of the zebrafish. *Dev Dyn*. 1995; 203:253–310. [PubMed: 8589427]
- Kwak EL, Bang YJ, Camidge DR, Shaw AT, Solomon B, Maki RG, Ou SH, Dezube BJ, Janne PA, Costa DB, et al. Anaplastic lymphoma kinase inhibition in non-small-cell lung cancer. *N Engl J Med*. 2010; 363:1693–1703. [PubMed: 20979469]
- Langenau DM, Keefe MD, Storer NY, Jette CA, Smith AC, Ceol CJ, Bourque C, Look AT, Zon LI. Co-injection strategies to modify radiation sensitivity and tumor initiation in transgenic Zebrafish. *Oncogene*. 2008; 27:4242–4248. [PubMed: 18345029]
- Lucas ME, Muller F, Rudiger R, Henion PD, Rohrer H. The bHLH transcription factor hand2 is essential for noradrenergic differentiation of sympathetic neurons. *Development*. 2006; 133:4015–4024. [PubMed: 17008447]
- Macdonald R. Zebrafish immunohistochemistry. *Methods Mol Biol*. 1999; 127:77–88. [PubMed: 10503226]
- Maris JM. Recent advances in neuroblastoma. *N Engl J Med*. 2011; 362:2202–2211. [PubMed: 20558371]
- Maris JM, Hogarty MD, Bagatell R, Cohn SL. Neuroblastoma. *Lancet*. 2007; 369:2106–2120. [PubMed: 17586306]
- Marusich MF, Furneaux HM, Henion PD, Weston JA. Hu neuronal proteins are expressed in proliferating neurogenic cells. *J Neurobiol*. 1994; 25:143–155. [PubMed: 7517436]
- Mierau GW, Weeks DA, Hicks MJ. Role of electron microscopy and other special techniques in the diagnosis of childhood round cell tumors. *Hum Pathol*. 1998; 29:1347–1355. [PubMed: 9865819]
- Molenaar WM, Baker DL, Pleasure D, Lee VM, Trojanowski JQ. The neuroendocrine and neural profiles of neuroblastomas, ganglioneuroblastomas, and ganglioneuromas. *Am J Pathol*. 1990; 136:375–382. [PubMed: 1689542]
- Morris SW, Kirstein MN, Valentine MB, Dittmer KG, Shapiro DN, Saltman DL, Look AT. Fusion of a kinase gene, ALK, to a nucleolar protein gene, NPM, in non-Hodgkin's lymphoma. *Science*. 1994; 263:1281–1284. [PubMed: 8122112]
- Mosse YP, Laudenslager M, Longo L, Cole KA, Wood A, Attiyeh EF, Laquaglia MJ, Sennett R, Lynch JE, Perri P, et al. Identification of ALK as a major familial neuroblastoma predisposition gene. *Nature*. 2008; 455:930–935. [PubMed: 18724359]
- Nilsson JA, Cleveland JL. Myc pathways provoking cell suicide and cancer. *Oncogene*. 2003; 22:9007–9021. [PubMed: 14663479]
- O'Brien EK, d'Alencon C, Bonde G, Li W, Schoenebeck J, Allende ML, Gelb BD, Yelon D, Eisen JS, Cornell RA. Transcription factor Ap-2alpha is necessary for development of embryonic melanophores, autonomic neurons and pharyngeal skeleton in zebrafish. *Dev Biol*. 2004; 265:246–261. [PubMed: 14697367]
- Palmer RH, Vernersson E, Grabbe C, Hallberg B. Anaplastic lymphoma kinase: signalling in development and disease. *Biochem J*. 2009; 420:345–361. [PubMed: 19459784]
- Pattyn A, Morin X, Cremer H, Goridis C, Brunet JF. The homeobox gene Phox2b is essential for the development of autonomic neural crest derivatives. *Nature*. 1999; 399:366–370. [PubMed: 10360575]

- Sasaki T, Okuda K, Zheng W, Butrynski J, Capelletti M, Wang L, Gray NS, Wilner K, Christensen JG, Demetri G, et al. The neuroblastoma associated F1174L ALK mutation causes resistance to an ALK kinase inhibitor in ALK translocated cancers. *Cancer Res.* 2010
- Stewart RA, Arduini BL, Berghmans S, George RE, Kanki JP, Henion PD, Look AT. Zebrafish foxd3 is selectively required for neural crest specification, migration and survival. *Dev Biol.* 2006; 292:174–188. [PubMed: 16499899]
- Stewart RA, Look AT, Kanki JP, Henion PD. Development of the peripheral sympathetic nervous system in zebrafish. *Methods Cell Biol.* 2004; 76:237–260. [PubMed: 15602879]
- Taxy JB. Electron microscopy in the diagnosis of neuroblastoma. *Arch Pathol Lab Med.* 1980; 104:355–360. [PubMed: 6893122]
- Teitelman G, Baker H, Joh TH, Reis DJ. Appearance of catecholamine-synthesizing enzymes during development of rat sympathetic nervous system: possible role of tissue environment. *Proc Natl Acad Sci U S A.* 1979; 76:509–513. [PubMed: 34153]
- Thisse C, Thisse B. High-resolution in situ hybridization to whole-mount zebrafish embryos. *Nat Protoc.* 2008; 3:59–69. [PubMed: 18193022]
- Tornoczky T, Semjen D, Shimada H, Ambros IM. Pathology of peripheral neuroblastic tumors: significance of prominent nucleoli in undifferentiated/poorly differentiated neuroblastoma. *Pathol Oncol Res.* 2007; 13:269–275. [PubMed: 18158560]
- Wessi WA, Aldape K, Mohapatra G, Feuerstein BG, Bishop JM. Targeted expression of MYCN causes neuroblastoma in transgenic mice. *Embo J.* 1997; 16:2985–2995. [PubMed: 9214616]

SIGNIFICANCE

Neuroblastoma is an important developmental tumor arising in the peripheral sympathetic nervous system, which accounts for ~10% of cancer-related deaths in childhood. The ALK receptor tyrosine kinase is mutationally activated in a subset of primary neuroblastomas, but the mechanisms through which ALK signaling cooperates with MYCN overexpression in neuroblastoma pathogenesis remain unclear. By generating a transgenic zebrafish model that overexpresses human *MYCN* and activated *ALK* in the fish analogue of the adrenal medulla, we now show that upregulated *MYCN* mediates sympathetic neuroblast hyperplasia, which is mitigated by a developmentally-timed apoptotic response. Activated ALK blocks neuroblast apoptosis at this critical time in development, establishing a mechanism for the synergistic relationship between these two oncoproteins in the pathogenesis of neuroblastoma.

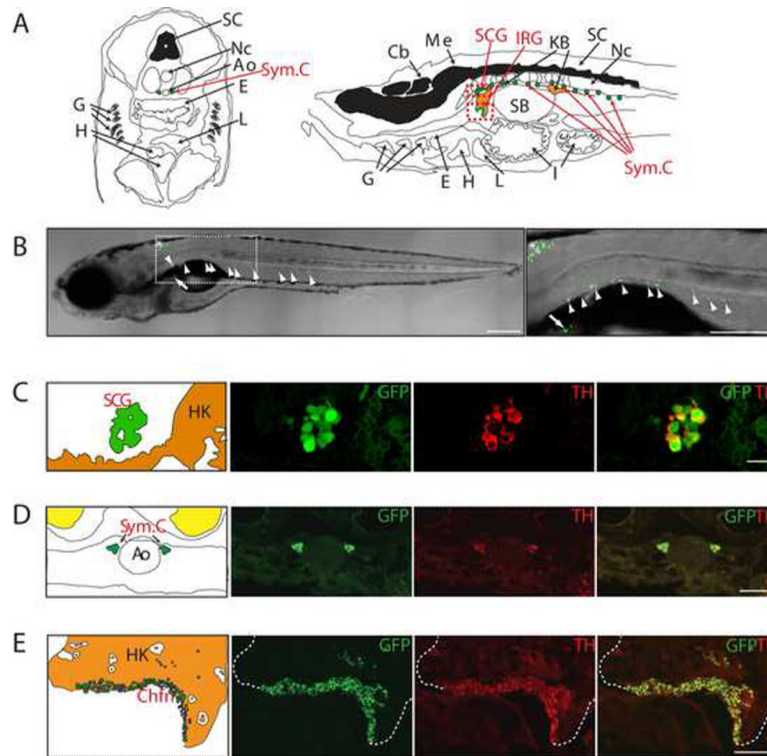


Figure 1. Transgenic gene expression in the sympathetic neurons and the interrenal gland

(A) *Left*: Schematic of a transverse section illustrating zebrafish anatomical structures, dorsal upwards. *Right*: Schematic of a sagittal section illustrating zebrafish anatomical structures, anterior to left.

(B) EGFP expression (green) in the zebrafish chain of sympathetic ganglia (arrowheads), the IRG (arrow) and medulla oblongata (asterisk) at 3 wpf. Lateral view of confocal-brightfield image, anterior to left. The magnified view of the boxed region is shown on the right. Scale bar, 500 μ m.

(C) EGFP is coexpressed with TH in the SCG at 6 wpf (sagittal section); TH coexpression is indicated in red. Scale bar, 20 μ m.

(D) EGFP is coexpressed with TH in the chain of sympathetic ganglia at 6 wpf (transverse section). TH coexpression is indicated in red. Scale bar, 20 μ m.

(E) EGFP is coexpressed with TH in the IRG at 8 months postfertilization (mpf) (sagittal section). TH coexpression is indicated in red. Scale bar, 100 μ m.

Ao, aorta; Cb, cerebellum; Chfn, chromaffin cells; E, esophagus; G, gill; H, heart; HK, head kidney; I, intestine; IRG, interregal gland; KB, kidney body; L, liver; Me, medulla; Nc, notochord; SB, swim bladder; SC, spinal cord; SCG, superior cervical ganglion; Sym.C, sympathetic chain.

See also Figure S1.

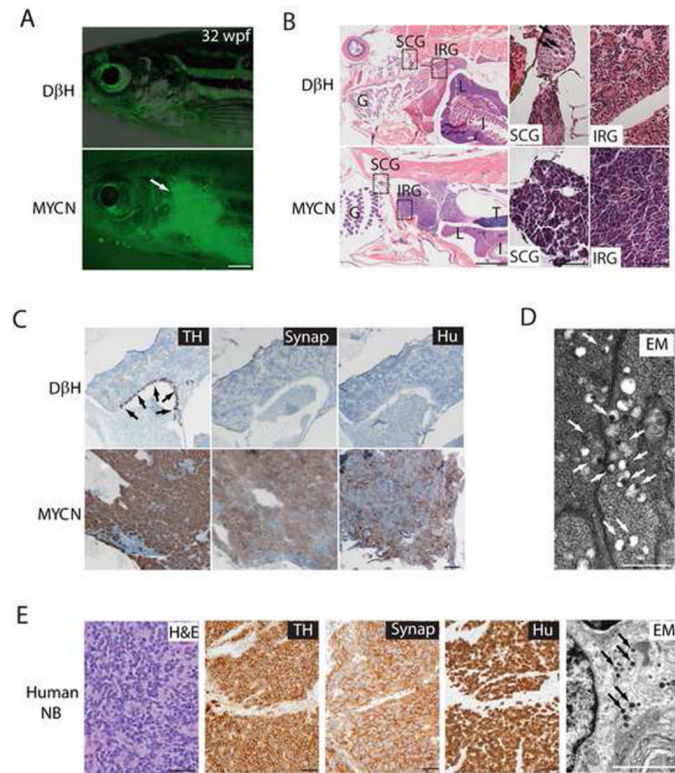


Figure 2. Neuroblastomas arise in *MYCN*-expressing transgenic zebrafish

(A) *Top*: D β H fish. *Bottom*: MYCN fish with EGFP-expressing tumor (arrow) at 32 weeks postfertilization (wpf). Scale bar, 1 mm.

(B) *Top*: H&E-stained sagittal sections of D β H fish. Boxes indicate the SCG and IRG, and are magnified in the right panels. *Bottom*: H&E-stained sagittal sections of MYCN fish with neuroblastic tumors. Boxes indicate the SCG and IRG and are magnified in the right panels. Arrows indicate SCG neurons. The majority of tumors arise in the IRG, although as seen in this example, tumor cells in the SCG were occasionally observed in individual fish that also had tumors in the IRG. G, gill; L, liver; I, intestine; IRG, interreginal gland; SCG, superior cervical ganglion; T, testis. Scale bar, 50 μ m.

(C) *Top*: Sagittal sections through the interreginal gland of D β H fish. Chromaffin cells of the interreginal gland express TH (arrows). *Bottom*: Sagittal sections through the interreginal gland of a MYCN fish with EGFP-expressing tumor. Cells throughout the tumor in the interreginal gland express TH, Synaptophysin (Synap) and Hu. Scale bar, 100 μ m.

(D) Electron microscopy (EM) reveals neurosecretory granules in the MYCN-expressing tumors (arrows). Scale bar, 500 nm.

(E) Pathological, immunohistochemical and ultrastructural analyses of a human neuroblastoma. Arrows point to neurosecretory granules. Scale bars, 500 μ m (left panel), 100 μ m (middle panels) and 2 μ m (right panel), respectively.

See also Figure S2.

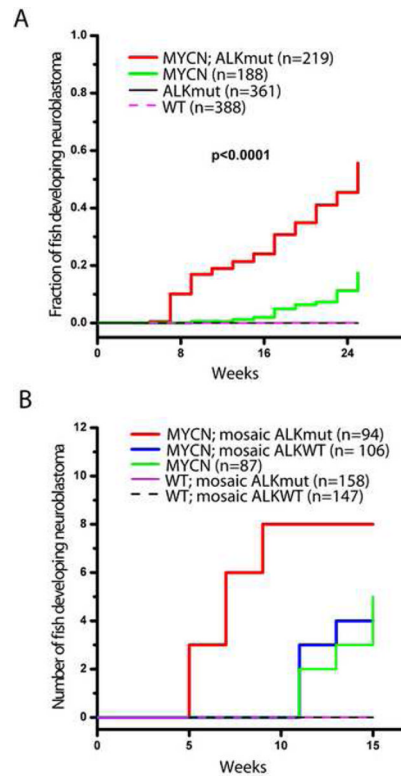


Figure 3. Activated ALK accelerates disease onset and increases the penetrance of MYCN-induced neuroblastoma

(A) Cumulative frequency of neuroblastoma in stable transgenic zebrafish by Kaplan-Meier analysis. ALKmut represents stable transgenic fish expressing the *ALK* (*F1174L*) transgene. WT, wild-type.

(B) Onset of neuroblastoma in MYCN transgenic fish or wild-type (WT) fish as mosaics coinjected with the following DNA constructs: i) *dβh-ALKF1174L* and *dβh-mCherry* (mosaic ALKmut), ii) *dβh-ALKWT* and *dβh-mCherry* (mosaic ALKWT), or iii) *dβh-mCherry* alone. The difference between tumor onset by 9 wpf in the MYCN fish coinjected with *dβh-ALKF1174L* and *dβh-mCherry* (MYCN; mosaic ALKmut) and that in the MYCN line coinjected with *dβh-ALKWT* and *dβh-mCherry* (MYCN; mosaic ALKWT) or *dβh-mCherry* alone (MYCN) is significant at $p=0.002$ and $p=0.007$, respectively, with two-tailed Fisher exact test.

See also Figure S3.

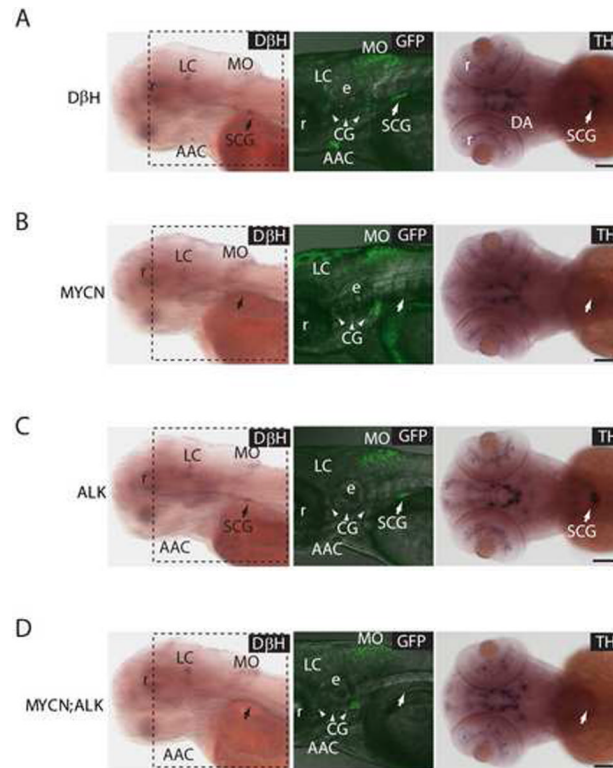


Figure 4. *MYCN* expression causes sympathoadrenal cell loss

(A) *DβH* transgenic line. Oblique views of *dβh* RNA expression (left panels); lateral views of EGFP expression in merged confocal-brightfield images (middle panels); dorsal views of *th* RNA expression (right panels). Arrows point to the SCG, and arrowheads point to the CG. Scale bar, 100 μ m.

(B) *MYCN* transgenic line. *MYCN* expression causes loss of cells in the SCG (arrows). Scale bar, 100 μ m.

(C) *ALK* transgenic line. *ALK* expression does not interfere with the SCG development (arrows). Scale bar, 100 μ m.

(D) *MYCN*;*ALK* transgenic line. Loss of cells in the SCG is not rescued by activated *ALK* expression (arrows). Scale bar, 100 μ m.

AAC, arch-associated catecholaminergic neurons; CG (arrowheads), cranial ganglia; DA, diencephalic dopaminergic neurons; e, ear; LC, locus coeruleus; MO, medulla oblongata; r, retina; SCG, superior cervical ganglion.

See also Figure S4 and Table S1.

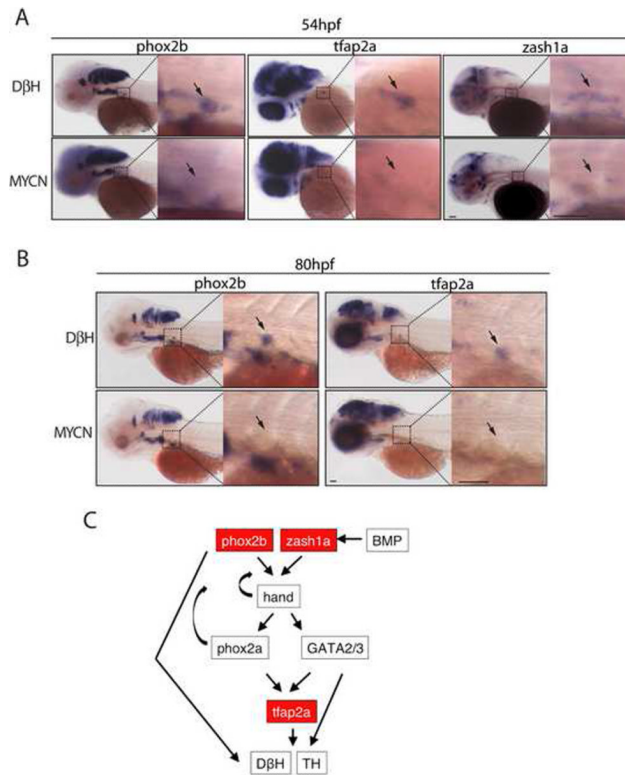


Figure 5. Expression of early sympathoadrenal markers is absent in MYCN transgenic embryos during early development

(A–B) Top panels: DβH; lower panels: MYCN transgenic fish. Expression of sympathoadrenal cell markers at 54 hpf (A) and 80 hpf (B). The magnified view of the boxed region is shown on the right. Arrows point to the superior cervical ganglion. Scale bars, 50 μm (left panels) and 100 μm (right panels, magnified view).

(C) Diagram of the genetic interactions of sympathoadrenal genes during early development. Arrows indicate the activation of target genes. Curved arrows indicate positive feedback regulation.

See also Figure S5.

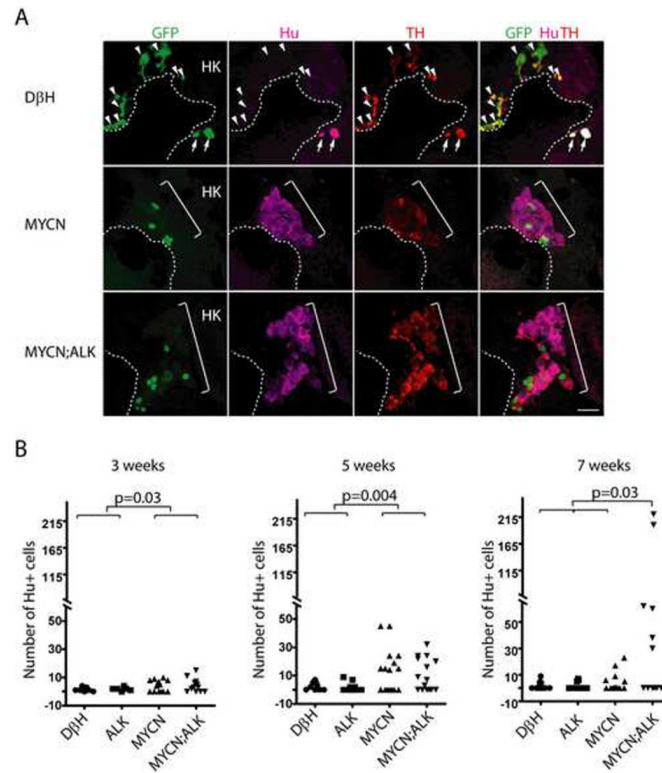


Figure 6. MYCN causes Hu+ cell hyperplasia in the interrenal gland

(A) Sagittal sections through the interrenal gland in DβH (top panels), MYCN (middle panels) and MYCN;ALK (lower panels) transgenic fish at 5wpf (dorsal up, anterior left). EGFP, green; Hu, magenta; TH, red. Representative sections through the interrenal gland in DβH fish contain 3–5 GFP+/Hu+/TH+ sympathetic neuroblasts (arrows) and many GFP+/Hu–/TH+ chromaffin cells (arrowheads). Hu+ cell numbers increase in MYCN and MYCN;ALK fish (brackets), and can be GFP+ and TH+. Dotted lines indicate the head kidney (HK) boundary. Scale bar, 20 μm.

(B) Numbers of Hu+ interrenal gland cells in DβH, ALK, MYCN and MYCN;ALK transgenic fish at 3, 5 and 7 weeks. Means of Hu+ cell numbers were compared by the two-tailed Wilcoxon signed-rank test.

See also Figure S6.

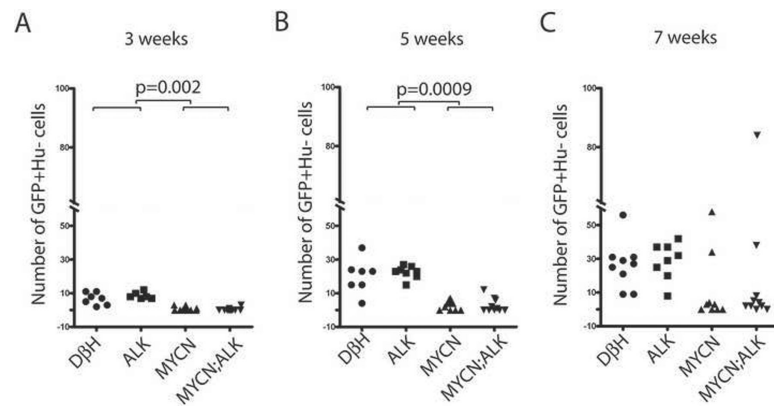


Figure 7. *MYCN* expression blocks chromaffin cell differentiation in the interrenal gland (A–C) Numbers of GFP+/Hu⁻ chromaffin cells in the interrenal gland in DβH, ALK, MYCN and MYCN;ALK transgenic fish at 3 weeks (A), 5 weeks (B) and 7 weeks (C). Means of GFP+/Hu⁻ cell numbers were compared by the two-tailed Wilcoxon signed-rank test.

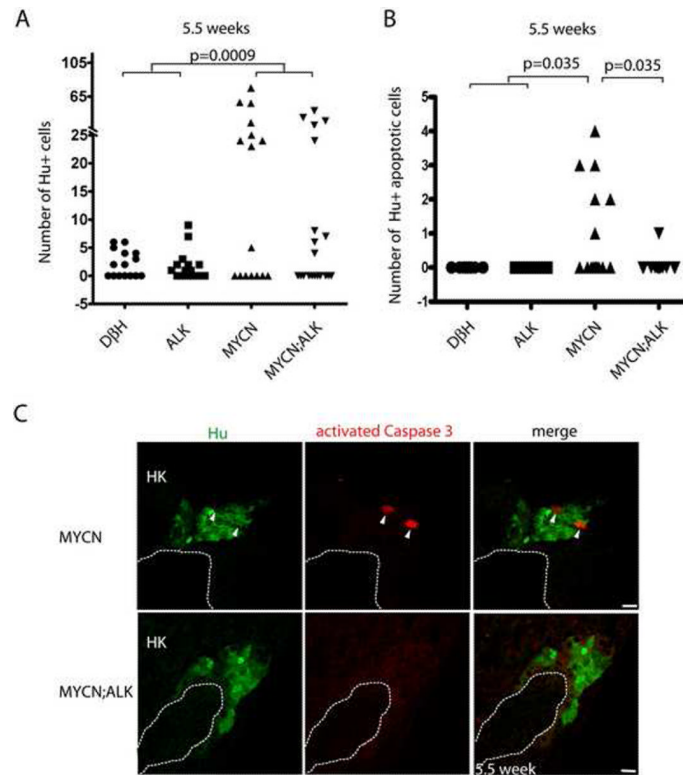


Figure 8. ALK inhibits a developmentally-timed apoptotic response triggered by MYCN overexpression in the interrenal gland

(A) Numbers of Hu+ interrenal gland cells in the DβH, ALK, MYCN and MYCN;ALK fish at 5.5 wpf. Means of Hu+ cell numbers were compared by the two-tailed Wilcoxon signed-rank test.

(B) Numbers of apoptotic Hu+ interrenal gland cells in the DβH, ALK, MYCN and MYCN;ALK fish at 5.5 wpf. The numbers of transgenic fish at 5.5 wpf with apoptotic Hu+ cells in the interrenal gland were compared by two-tailed Fisher exact test.

(C) Sagittal sections through the interrenal gland in MYCN (top panels) and MYCN;ALK (bottom panels) transgenic fish at 5.5 wpf (dorsal up, anterior left). Hu, green; activated Caspase-3, red. Hu+, activated Caspase-3+ apoptotic cells were detected in the MYCN transgenic fish (arrowheads). Dotted lines indicate the head kidney (HK) boundary. Scale bars, 10 μm.

See also Figure S7.